Hindawi Publishing Corporation
Advances in Physical Chemistry
Volume 2012, Article ID 720197, 17 pages
doi:10.1155/2012/720197

Review Article

Potential Energy Surfaces for Reactions of X Metal Atoms (X = Cu, Zn, Cd, Ga, Al, Au, or Hg) with YH_4 Molecules (Y = C, Si, or Ge) and Transition Probabilities at Avoided Crossings in Some Cases

Octavio Novaro,[1] María del Alba Pacheco-Blas,[1] and Juan Horacio Pacheco-Sánchez[2]

[1] *Instituto de Física, Universidad Nacional Autónoma de México, A.P. 20-364, 01000 Ciudad de México, DF, Mexico*
[2] *División de Estudios de Posgrado e Investigación, Instituto Tecnológico de Toluca, A.P. 890, 52140 Metepec Edo. Mex, Mexico*

Correspondence should be addressed to Octavio Novaro, novaro@fisica.unam.mx

Received 14 July 2011; Revised 4 October 2011; Accepted 22 November 2011

Academic Editor: Laimutis Bytautas

We review *ab initio* studies based on quantum mechanics on the most important mechanisms of reaction leading to the C–H, Si–H, and Ge–H bond breaking of methane, silane, and germane, respectively, by a metal atom in the lowest states in C_s symmetry: X(2nd excited state, 1st excited state and ground state) + YH_4 → H_3XYH → H + XYH_3 and XH + YH_3. with X = Au, Zn, Cd, Hg, Al, and G, and Y = C, Si, and Ge. Important issues considered here are (a) the role that the occupation of the d-, s-, or p-shells of the metal atom plays in the interactions with a methane or silane or germane molecule, (b) the role of either singlet or doublet excited states of metals on the reaction barriers, and (c) the role of transition probabilities for different families of reacting metals with these gases, using the H–X–Y angle as a reaction coordinate. The breaking of the Y–H bond of YH_4 is useful in the production of amorphous hydrogenated films, necessary in several fields of industry.

1. Introduction

Here, an overview of potential energy surface (PES) calculations for reactions of a metal atom with a gas molecule has been compiled. Among metal atoms, we consider cadmium, copper, zinc, gallium, aluminum, mercury, and gold, and among gas molecules methane, silane, and germane. The potential energy surfaces of an YH_4 molecule with a metal atom were determined using *ab initio* Hartree-Fock Self-Consistent Field (HF-SCF) calculations, where the atom core is represented by relativistic effective core potentials (RECPs) [1–5]. These calculations are followed by a Multi-configurational Self Consistent Field (MC-SCF) study [6]. The correlation energy is accounted for through extensive variational and perturbative second-order multireference Moller-Plesset configuration interaction (MR-CI) analysis of selected perturbations obtained by iterative process calculations using the CIPSI program package [7]. The reference (S) spaces used for the variational CI of the molecular states arising from the three X + CH_4 asymptotes contain between 108 and 428 determinants, which generate between 7 million and 111 million perturbed MP2 determinants near the region of the reactants and the equilibrium geometry of the methyl-metal-hydride intermediate, respectively. This methodology is particularly useful in the study of systems constituted by a few atoms.

Transition probabilities for the interaction of the lowest excited states of the metal X with tetrahedral gas molecules are studied through one-dimensional Landau-Zener theory. The strategy for obtaining the reaction pathways for X + YH_4 interactions has been extensively used in references [8–14] based on the original proposal by Chaquin et al. [15]. The initial approach (starting from 20 a.u.) of the X atom to one Y–H bond was done in a C_s symmetry in a plane containing the X, Y, and two hydrogen atoms. All the angles and distances obtained by a self-consistent field approach to

find the molecular geometry of the $HXYH_3$ intermediate are exhibited in Figure 1. From these parameters, θ = H–X–Y is the first angle fixed in order to optimize the other angles and distances for each point on a potential energy curve, and taking steps of 10 degrees for the θ angle. When two energy levels cross each other as a function of time, the semiclassical theory of time-dependent Landau-Zener theory [16, 17] for nonadiabatic transition can be utilized. Zener [17] proposed a transition probability from one potential energy curve to another as a linear velocity function, using the distance r as the reaction coordinate. Whereas for an angular velocity using the angle θ as the reaction coordinate, all developments established by Zener are still valid, given that for determining a time-dependent transition probability, the Schrödinger equation must be used. Thus, the transition probability from one-potential energy curve to another is an angular velocity function, using the angle θ as the reaction coordinate. Our theoretical results predict the formation of XH + YH_3 or H + XYH_3 products after breaking the intermediate $HXYH_3$. Some of these products are useful in the industry to get hydrogenated amorphous films (a-Y : H) among the other applications [18–30].

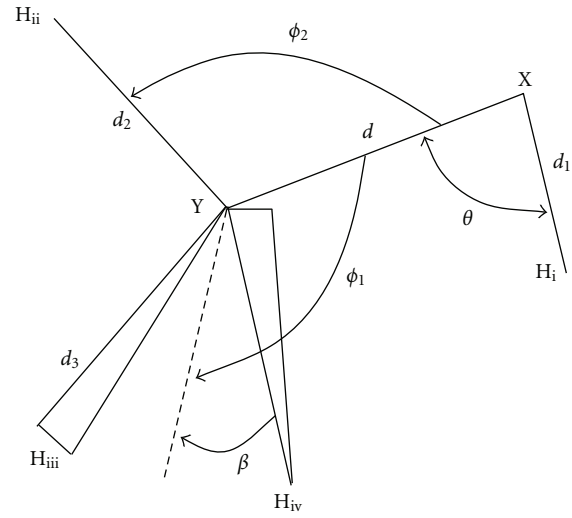

Figure 1: The eight (θ, ϕ_1, ϕ_2, β, d, d_1,d_2, and d_3) geometrical parameters used for the optimal X + YH_4 reaction pathway.

The complexity of the organometallic systems, aggregates, and metallic surfaces makes it difficult to determine the fundamental mechanisms which govern their interactions with hydrocarbons. In this situation, one begins with a study of the interaction of a single metallic atom with a hydrocarbon molecule as a model to understand the conditions that the metallic center in these activations requires. Thus, the study of the interaction of the different metallic atomic states with the methane, silane, or germane molecule is fundamental in elucidating the role of various d-, s-, or p-orbital occupations in a metal atom.

Experimental studies [31–38] carried out on the photolysis induced by the metallic atom excitation in a matrix of methane at low temperatures show that when the C–H bond of methane activates through photoexcited metallic atoms deposited in a matrix at low temperatures, the process only happens with radiation wavelengths previously known to be absorbed in the free atom, allowing it to achieve a transition to an excited state. The very low temperature of the matrix fixes the position and also reduces the internal movements of methane molecules contained in it, allowing the interaction of C–H bonds with deposited metallic atoms.

The photochemical studies on the metal-alkane interaction have attracted the attention of researchers for long time. It is worth mentioning that in 1985 the work entitled "Activation of Methane by Photoexcited Copper Atoms and Photochemistry of Methylcopper Hydride in Solid Methane Matrices," developed in Lash Miller laboratories of the University of Toronto in Canada by the G.A Ozin group [32] was considered in the publication analysis of Scientific Information Institute (current contents) as the most promising work of that year.

At room temperature and standard pressure, methane (CH_4) is a colorless, odorless, and flammable gas [39], in fact the simplest hydrocarbon. It is the major constituent of natural gas and is released during the decomposition of plants or other organic compounds, as in marshes and coal mines. Methane is the first member of the alkane series. The strength of the carbon hydrogen covalent bond in methane is perhaps the strongest in all hydrocarbons, and, thus, its use as a chemical feedstock is limited. Despite the high activation barrier for breaking the C–H bond, CH_4 is still the main starting material for manufacture of hydrogen in steam reforming. The search for catalysts which can facilitate C–H bond activation in methane (105 kcal mol^{-1} to break it) and other low alkanes is an area of research with considerable industrial significance [40].

Silane is a chemical compound (SiH_4) analogous to methane, and it is also a gas at room temperature which undergoes spontaneous combustion in air. The name "silane" is also given to a family of compounds that are silicon analogs of alkane hydrocarbons. The radical SiH_3 is termed silyl. The nomenclature parallels that of alkyl radicals. Silane may also carry certain functional group, just as alkanes do. There is (at least in principle) silicon analog for each carbon alkane. Silanes are useful for several industrial and medical applications. For instance, they are used as coupling agents to adhere glass fibers to a polymer matrix, stabilizing the composite material. They can also be used to couple a bioinert layer on a titanium implant. Other applications include water repellents, masonry protection, control of graffiti, applying polycrystalline silicon layers on silicon wafers when manufacturing semiconductors, and sealants. In addition, silane and similar compounds containing Si–H bonds are used as reducing agents in organic and organometallic chemistry [41–47].

Germane is the chemical compound with the formula GeH_4, and an analog of methane. It is the simplest germanium hydride and one of the most useful compounds of germanium. Like the related compounds silane and methane, germane is tetrahedral. It burns in the air to produce GeO_2 and water. Some processes for the industrial manufacture of germane [48], in which our calculations might be useful, are (a) chemical reduction method, (b) an electrochemical

reduction method, and (c) a plasma-based method. The gas decomposes near 600 K to germanium and hydrogen. Germane is used in the semiconductor manufacturing for epitaxial growth of germanium [49]. Organogermanium precursors have been examined as less hazardous liquid alternatives to germane for deposition of Ge-containing films [50]. Germane is flammable and toxic.

The quantum chemistry studies presented here provide valuable information about the activation of methane or silane or germane molecules with metal atoms. Products of these reactions are methyl CH_3 or silyl SiH_3 or germyl GeH_3 radicals, which are key in surface growth of amorphous hydrogenated carbon or silicon or germane films (thin films).

Methane CH_4, silane SiH_4, and Germane GeH_4 species turn out to be valuable substances in the industry of the semiconductors since the germane or silane or methane dehydrogenation in gaseous phase is one of the most current methods to obtain semiconductors in the form of amorphous hydrogenated carbon (*a*-C : H) [51] or silicon (*a*-Si : H) [52] or germane (*a*-Ge : H) [53] thin films. The interaction of CH_3, SiH_3, or GeH_3 radicals and atomic hydrogen with the surfaces of carbon, silicon or germane films *a*-C : H, *a*-Si : H, or *a*-Ge : H plays a fundamental role in the understanding of the growth of these plasma films at low temperature. Street [54] says that the dehydrogenated material has a very high defect density which prevents doping, photoconductivity, and the other desirable characteristics of a useful semiconductor. While a real crystal contains defects such as vacancies, interstitial, and dislocations, the elementary defect of an amorphous semiconductor is the coordination defect, when an atom has too many or too few bonds [54]. Defect equilibrium is in general described by a reaction of the type

$$\mathrm{A} + \mathrm{B} \leftrightarrows \mathrm{C} + \mathrm{D}, \tag{1}$$

where A–D are different configurations of point defects, dopants, electronic charges, and so forth. The properties of interest are the equilibrium state and the kinetics of the reaction [54]. Calculations as those accomplished by us mentioned previously might help to find these properties. As an example, our calculated energy of the intermediate corresponds to the defect formation energy U_d which determines the equilibrium defect density, as part of the kinetics of reaction.

Methyl radical absorption on carbon or hydrocarbon thin films is key in thin-film growth at low-temperature plasmas ($< T_{\mathrm{room}}$) using hydrocarbon precursor gases.

The current production procedure of amorphous hydrogenated carbon (*a*-C : H) or silicon (*a*-Si : H) films is the deposition by means of the decomposition of methane or silane through glow discharges produced by radio frequency (RF). This method is known as plasma-enhanced chemical vapor deposition (PECVD) [55].

The breaking of the C–H bond of CH_4 is useful for generating amorphous hydrogenated carbon (*a*-C : H) films, which represent a class of high-technology materials with mechanical, optical, chemical, and electrical properties among polymeric, graphite, and diamondoid films.

The (*a*-C : H) is of interest to the electronic industry as a viable and cheap semiconductor that can be prepared in an ample rank of layers. The fine layer of *a*-C : H, also well-known as diamondoid carbon, is used as a revesting material of hard and low friction. The polymeric film *a*-C : H has a strong photoluminescence and is being developed as an electroluminescent material. It is also used as dielectric in metal-insulator-metal switch in screens of active matrix. The ability of deposition near to room temperatures using cheap methods of chemical vapor deposition (CVD) makes this material useful for the industry. The amorphous nature of these materials and their relative facility of deposition make them ideals for its use in a great amount of applications such as in panels of flat screen and diamondoid technology [56].

The *a*-C : H films are prepared through a glow discharge of RF in a pure methane atmosphere at different gas pressures in which the methane decomposition generates the methyl CH_3 radical, which plays a preponderant role in the generation of amorphous hydrogenated carbon surfaces [57, 58]. The electronic industry takes profit of the previous proceeding on the formation of diamondoid films.

Dense amorphous hydrocarbons have some of the highest densities among hydrocarbon and fall between crystalline diamonds and adamantanes, according to Angus [59]; this is the property that makes it so attractive to the electronic industry.

In case of diamondoid formation,

(1) some excited metallic atoms break the C–H bond of methane with the consequent production of methyl CH_3 radicals [8, 60, 61]. Knowing that a dangling bond is an unsatisfied valence on an immobilized atom, the methyl CH_3 radicals undergo a chemisorption process controlled by the creation of dangling bonds in the *a*-C : H surface by an atom H. This is a proper process in the formation of diamondoid films in the electronic industry [62],

(2) Ramĺrez and Sinclair [63] (and Velasco-Santos et al., [64]) affirm that carbonaceous natural products can have different allotropic forms of the carbon, since the amorphous carbon has graphite transitions at different temperatures when some specific metals are in contact with carbon and act as catalysts,

(3) methyl CH_3 radicals can also be generated by photodissociation of aromatic hydrocarbon, consequently amorphous hydrogenated carbon thin films can be produced. Taguchi et al. [65] used two classes of laser (ArF or KrF) and two types of aromatics (benzene C_6H_6 or toluene C_6H_5–CH_3) to generate diamondoid films.

The breaking of Si–H bond of SiH_4 is useful in manufacture of semiconductor films of amorphous hydrogenated silicon (*a*-Si : H). Before the *a*-Si : H material has been developed, the research was on amorphous silicon without hydrogen, prepared by sputtering or by thermal evaporation.

There are at least two models for the generation of amorphous hydrogenated silicon (*a*-Si : H).

(i) In the thermodynamic approach [62, 66, 67], the formation of dangling bonds, the principle defect in *a*-Si:H, is attributed to the breaking of weak Si–Si bonds caused by mobile H that is released from Si–H bonds [68]:

$$\text{H} + \text{weak bond} \longleftrightarrow \text{Si–H} + \text{broken bond}. \quad (2)$$

(ii) In the Matsuda-Gallagher-Perrin MGP model [66, 67], SiH_3 *is assumed to be the only growth precursor. This assumption is based on the (presumed) dominance of this radical in plasmas leading to the device-quality* *a*-Si : H.

The central assumption in the MGP model is that the SiH_3 reaching the *a*-Si : H can go to a weakly adsorbed (physisorbed) state forming a three-center Si–H–Si bond on a surface Si–H site. The activation of silane molecules has received a lot of attention as much in the experimental aspect [61, 69–72] as in the theoretical [9, 73]. The activation of the Si–H bond is important as much in the processes of polymerization of silane [74, 75], as in organometallic catalytic reactions [76–78].

The growth of amorphous hydrogenated silicon films *a*-Si : H in silicon substrata through PECVD in silane is widely used in the manufacture of electronic, optoelectronic, and photovoltaic devices. Amorphous semiconductors of thin films are used in an ample variety of applications such as solar cells, TFT, photoreceptors, and apparatus of images [79].

The *a*-Ge : H films are prepared through a glow discharge of RF in a pure germane atmosphere at different gas pressures in which the germane decomposition generates the germyl GeH_3 radical, which plays a preponderant role in the generation of amorphous hydrogenated germane surfaces [53].

Here we stress some important results at metal-methane, metal-silane, and metal-germane interactions grouped in three different families (coinage metals: Cu and Au. Pseudo-transition metals: Zn, Cd, and Hg, and metals: Al and Ga). Castillo et al. [8, 60, 80] carried out calculations of potential energy surfaces of the interactions copper methane and zinc methane with the aim of determining the mechanisms of reaction that involve the three lowest states of the copper atom (^{2}S, ^{2}D, and ^{2}P) as well as to determine the reaction routes that govern the interaction of the three lowest states of the zinc atom (^{1}S, ^{3}P, and ^{1}P) in the process of the C–H bond activation of the methane molecule. Luna-García et al. [11, 12, 81] found the interaction potential curves of the mercury-Germane, cadmium-Germane, copper-silane, and copper-germane in the three lowest states of each metal; he improved a computational methodology to get the products of the breaking of the intermediate. Pacheco-Sánchez et al. [13, 14, 40] achieved the calculation of gallium-methane and gallium-silane interactions as much in the ground state as in the two lowest excited states of gallium; he extended Landau-Zener theory [82–85] to use the angle instead of the distance as reaction parameter in transition probability calculations at avoided crossings. Transition probability theory is described here when the reaction parameter is distance or angle. In addition, our group has considered also the following interactions: cadmium methane [86], zinc silane [9], cadmium silane [10], mercury silane [9], gold silane [87], and recently aluminum methane [88].

2. Transition Probability Theory

When two potential energy curves are very near to each other, it seems that they crossover. Actually, in the apparent crossover point, the system is degenerate, since the two different electronic configurations have the same energy [89]. This introduces a resonance energy that separates the surfaces slightly, in such way that they never intersect but only closely approach to each other before repelling. Whereas the wave function of the molecule in a given curve is of one character before the crossing point (CP) and of another character after it, the wave function of the other curve is reversed in turn; an example is given in Figure 2, where we can see that while the wavefunction ψ_1 has $6p^1$ character before CP at ξ_0 and $6s^1$ character after CP at ξ_0, the wavefunction ψ_2 has $6s^1$ character before CP at ξ_0 and $6p^1$ character after CP at ξ_0. If ξ changes with a finite velocity, the probability that the molecule changes of a wave function to the other when passing through the crossing point is in such way that its electronic state is represented by a linear combination of the type

$$\psi = A_1(\xi)\psi_1 + A_2(\xi)\psi_2, \quad (3)$$

where $\xi = r$ or $\xi = \theta$ according to the reaction coordinate in study. By convenience in the calculation of A_1 and A_2, the eigenfunctions ψ_1 and ψ_2 are expressed in terms of two other wave functions φ_1 and φ_2 with energies ϵ_1 and ϵ_2, respectively, which intersect when they are plotted as functions of the internuclear distance (or angle). Due to the fact that φ_1 and φ_2 are not exact eigenfunctions of the whole Hamiltonian at the crossing point, the interaction energy ϵ_{12} between the two states φ_1 and φ_2 have to be included, then $E_1 = \epsilon_1 - \epsilon_{12}$ and $E_2 = \epsilon_2 + \epsilon_{12}$, where ϵ_{12} is the difference between the exact eigenvalues E_1 and E_2 and the approximate eigenvalues ϵ_1, ϵ_2: $\epsilon_{12}(\xi_0) = (E_1(\xi_0) - E_2(\xi_0))/2$. Normalizing and orthogonalizing all the wavefunctions involved, and following the one-dimensional (distance as reaction coordinate) developments established by Zener [17] for a time-dependent Schrödinger equation, we obtain the transition probability as

$$P = e^{-2\pi\gamma}, \quad (4)$$

where

$$\gamma = \frac{2\pi}{h}\frac{\epsilon_{12}^2}{|(d/dt)(\epsilon_1 - \epsilon_2)|^2}. \quad (5)$$

The denominator can be expressed as

$$\left|\frac{d}{dt}(\epsilon_1 - \epsilon_2)\right| = \eta\left|\frac{\partial\epsilon_1}{\partial\xi} - \frac{\partial\epsilon_2}{\partial\xi}\right| = \eta|s_1 - s_2|, \quad (6)$$

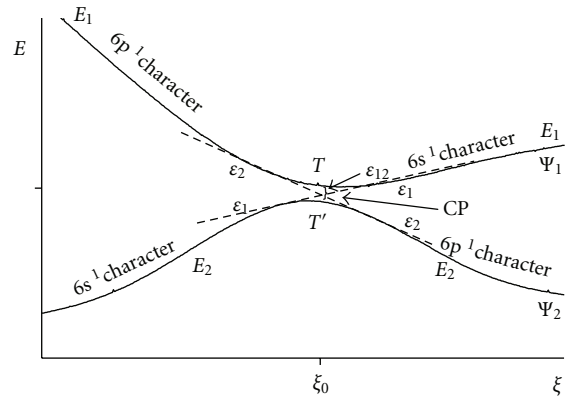

FIGURE 2: Typical graph of transition probabilities. Energy as a function of the insertion angle θ, where the two *solid lines* correspond to the avoided crossing at ξ_0, and the *dashed lines* to the probable transitions among potential energy surfaces.

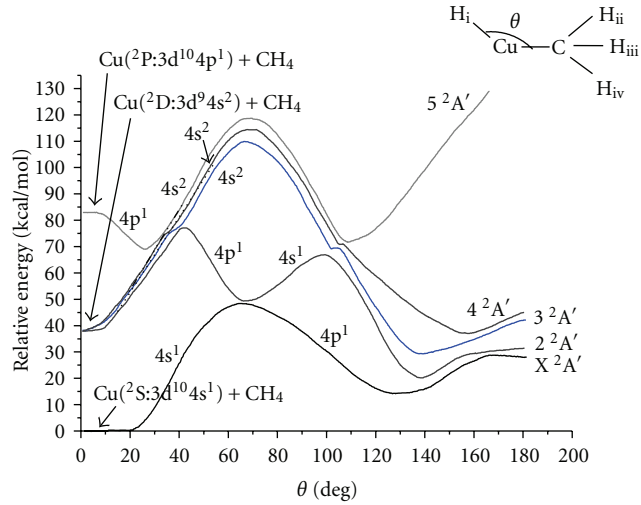

FIGURE 3: Insertion mechanism of the three lowest states of the Cu atom (^{2}S, ^{2}P, and ^{2}D) into a C–H bond of methane. ^{2}A′ interaction energy states as a function of the angle theta. The 4p^1 character follows the path from the second excited state to the minimum in the X A′ state, where the final products are formed.

where $\eta = d\xi/dt$ is the velocity ($\eta = v$ or $\eta = \omega$, v means linear and ω means angular velocity) at which the system crosses $\xi = \xi_0$, and $|s_1 - s_2|$ is the difference of the slopes of the two potential surfaces crossing at ξ_0. Finally, we have

$$P = e^{-(4\pi^2\epsilon_{12}^2/h\eta|s_1-s_2|)} \tag{7}$$

for the transition probability of nonadiabatic behavior. The probability for a system remaining in the initial energy surface is then

$$P' = 1 - e^{-(4\pi^2\epsilon_{12}^2/h\eta|s_1-s_2|)}. \tag{8}$$

Rosenkewitsch [90] states that Zener [17] has obtained a similar formula to that one obtained by Landau [16] (or (7) above)

$$P \approx e^{-(\pi/2h\upsilon)(\Delta^2/F_1-F_2)}, \tag{9}$$

where $\Delta = 2\epsilon_{12}$, υ is the relative velocity, and F_1 and F_2 are "forces" acting on the two states. Making the identification $d/dt(\epsilon_1 - \epsilon_2) = \upsilon(F_1 - F_2)$ which corresponds to the change of pure kinetics energy with time, we can almost have the equation found by Zener ((7) when $\eta = v$), because the exponent of the Landau formula also has a factor of 2π.

Explicit calculations of transition probabilities of nonadiabatic behavior using (7) are straightforward when the reaction coordinate is the distance [91, 92] (in these cases gas is hydrogen and metal is ruthenium [91] and platinum [92]); however, when the latter is the angle, it will be necessary to calculate the angular velocity and the moment of inertia as accomplished in references [40, 82–85, 87, 88] for tetrahedral molecules interacting with metals.

2.1. Interactions of the Cu, Au Coinage Metals with YH_4. Castillo et al. [60] found that copper in its second excited state (^{2}P: 3d^{10} 4p^1) breaks the C–H bond of methane, and its avoided crossing with the first excited state allows (^{2}D: 3d^9 4s^2) to surpass a barrier of 48 kcal mol^{-1}. We have a transition energy of ~83 kcal mol^{-1} between the states ^{2}P and ^{2}D and transition energy of ~43 kcal mol^{-1} between the states ^{2}D and ^{2}S (see Table 1 and Figure 3). Transition probability (TP) values at four avoided crossings [82] are obtained when copper is photoexcited to this second excited state Cu (^{2}P: 3d^{10} 4p^1), given that this copper atom is inserted in the methane molecule. It is also noteworthy [60] that the ground state is initially repulsive, but due to the avoided crossings, it became attractive after surmounting a rather high barrier. This behavior is initially exhibited at the first minimum (69 kcal mol^{-1}, 26°) of the 5 ^{2}A′ state forming the $HCuCH_3$ intermediate, which when continuing its path has a probability $P = 0.68$ of crossing towards the 4 ^{2}A′ state with 4p^1 character and a probability $P = 0.32$ of continuing by the same 5 ^{2}A′ state with 4s^2 character. When following via 4 ^{2}A′ has a probability $P = 0.61$ of crossing towards the 3 ^{2}A′ state with 4p^1 character and a probability $P = 0.39$ of continuing by the same 4 ^{2}A′ state with 4s^2 character. When continuing via 3 ^{2}A′, a very small potential barrier is surmounted with a probability $P = 0.65$ of crossing towards the 2 ^{2}A′ state with 4p^1 character, and a probability $P = 0.35$ of continuing by the same 3 ^{2}A′ state with 4s^2 character. When continuing via 2 ^{2}A′, it descends until reaching X ^{2}A′, then it has a probability $P = 0.62$ of crossing towards the X ^{2}A′ state with 4p^1 character and a probability $P = 0.38$ of continuing by the same 2 ^{2}A′ state (see Figure 3) with 4s^1 character. Finally, when continuing via X ^{2}A′ state (with 4p^1 character), while the theoretical energy of the $HCuCH_3$ intermediate is 14 kcal mol^{-1}, the experimental energy is between 15 and 25 kcal mol^{-1}. From here we can build the corresponding potential energy surfaces leading to the products by calculating the energy against the distance [60]. These products are H + $CuCH_3$ and HCu + CH_3, with theoretical energies 52 and 41 kcal mol^{-1}, respectively, and experimental energy values 46 and 40 kcal mol^{-1}, respectively, as mentioned in Table 1.

Pacheco-Sánchez et al. [87] have found that Gold in its second excited state (^{2}P: 5d^{10} 6p^1), through a series

Table 1: Coinage metal family (Cu, Au). Relative energies (kcal mol^{-1}) of the reactants, intermediary $HXYH_3$ and final products for three states of the metal. X(2nd): metal in second excited state. X(1st): metal in first excited state. X(gs): metal in ground state. ΔE_{Exp}: experimentally measured energy. ΔE_{Cal}: theoretically calculated energy.

X: Metal	Y: Methane		Y: Silane				Y: Germane	
	Cu[a] (^{2}S, ^{2}D, ^{2}P)		Au[b] (^{2}S, ^{2}D, ^{2}P)		Cu[c] (^{2}S, ^{2}D, ^{2}P)		Cu[c] (^{2}S, ^{2}D, ^{2}P)	
	ΔE_{Exp}	ΔE_{Cal}	ΔE_{Exp}	ΔE_{Cal}	ΔE_{Exp}	ΔE_{Cal}	Exp[d]	Cal.
X(2nd) + YH_4	85	~83	114.3	109.8	87.8	87.7	87.8	87.7
X(1st) + YH_4	34.9	~43	40.23	41.5	34.4	39.0	34.4	39
H + XYH_3	46	52[a]		30.91		36.0		33.2
HX + YH_3	40	41[a]	18.25	21.9	27.7	33.2	21.7[e]	27.1
$HXYH_3$	15–25	14[a]		3.34		5.8		1.6
X(gs) + YH_4	0	0	0	0	0	0	0	0

[a]From [80]
[b]From [87]
[c]From [12]
[d]From [93]
[e]From [94].

of avoided crossings that diminish the barriers for the ground state and first excited state, breaks the Si–H bond of silane, finally overcoming a barrier of 24.0 kcal mol^{-1} of the ground state. The experimental transition energy between the excited state (^{2}P: $5d^{10}$ $6p^1$) and the ground state (^{2}S: $5d^{10}$ $6s^1$) is 114.28 kcal mol^{-1}, which is comparable to the transition energy of 109.8 kcal mol^{-1} calculated by Pacheco-Sánchez et al. (Table 1). Then, the $HAuSiH_3$ intermediate encounters four avoided crossings between trajectories C ^{2}A′, B ^{2}A′, A ^{2}A′, and X ^{2}A′ of the energy surfaces. When gold is photoexcited to its second excited state ^{2}P: $5d^{10}$ $6p^1$, it initially passes through the avoided crossing around (77 kcal mol^{-1}, 28°) of D ^{2}A′ state, and there are two possibilities of the intermediate formed for following a trajectory. Taking it to pass the avoided crossing, it has a probability $P = 0.802$ [87] for crossing towards C ^{2}A′ maintaining the $6p^1$ character, where it finds another avoided crossing, and there is a probability of 0.737 for crossing toward B ^{2}A′ also maintaining the $6p^1$ character. Here it finds another avoided crossing, and there is a probability of 0.803 of crossing toward the A ^{2}A′ still maintaining the $6p^1$ character (see Figure 4). Henceforth, it finds the last avoided crossing, and there is a probability of 0.541 of crossing to the X ^{2}A′ maintaining the $6p^1$ character too, where the products are reached at 120°. Finally, the intermediate with energy 3.34 kcal mol^{-1} evolves toward the HAu + SiH_3 and $AuSiH_3$ + H products, whose energies are 21.9 and 30.91 kcal mol^{-1}. These products are of greater energy than the reactants, something typical in an endergonic reaction in which the reaction requires absorption of energy.

Luna-García et al. [12] have found that copper in its second excited state (^{2}P: $3d^{10}$ $4p^1$) breaks the Si–H bond of silane, in a manner quite similar to the previous cases surpasses a barrier of 26.0 kcal mol^{-1} of the ground state. The experimental transition energy between the excited state (^{2}P: $3d^{10}$ $4p^1$) and the ground state (^{2}S: $3d^{10}$ $4s^1$) is 87.8 kcal mol^{-1}, which agrees with the transition energy

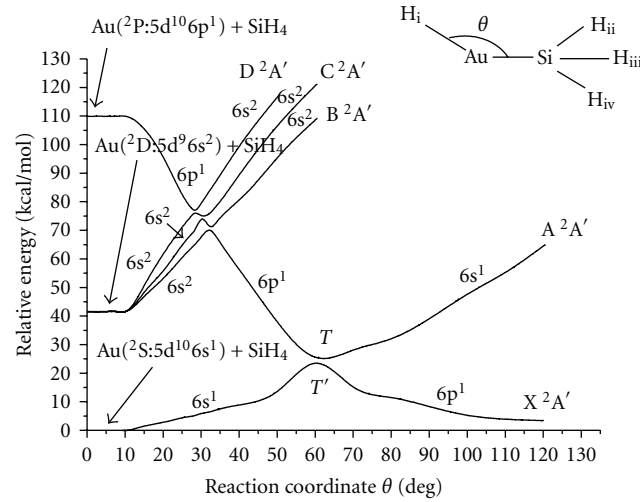

Figure 4: Au (^{2}S, ^{2}P, and ^{2}D) with SiH_4 interaction potential energy curves versus the θ insertion angle towards the $HAuSiH_3$ intermediate product. The $6p^1$ character follows the path from the second excited state to the minimum in the X ^{2}A′ state, where the final products are formed.

of 87.7 kcal mol^{-1} theoretically calculated (Table 1). The initial formation of the $HCuSiH_3$ intermediate starts at the minimum (70 kcal mol^{-1}, 20°) with $4p^1$ character and encounters four avoided crossings among trajectories 4 ^{2}A′, 3 ^{2}A′, 2 ^{2}A′, and X ^{2}A′ of the energy surfaces (see Figure 5). Finally, due to the endergonic nature of this reaction, the intermediate with energy 5.8 kcal mol^{-1} (and $4p^1$ character) is divided into the HCu + SiH_3 and $CuSiH_3$ + H products with theoretical energy values of 33.2 and 36.0 kcal mol^{-1}, respectively (see Table 1). In the same Table, we could only report the experimental energy value 27.7 kcal mol^{-1} of HCu + SiH_3 products.

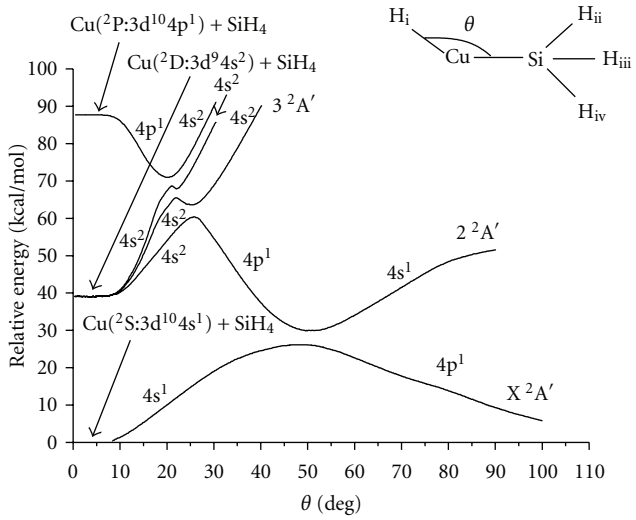

FIGURE 5: Potential energy curves of the Cu(^{2}S, ^{2}D, ^{2}P) interaction with SiH_4 as a function of the insertion angle (θ) towards the $HCuSiH_3$ intermediate product. The $4p^1$ character follows the path from the second excited state to the minimum in the X ^{2}A′ state, where the final products take place.

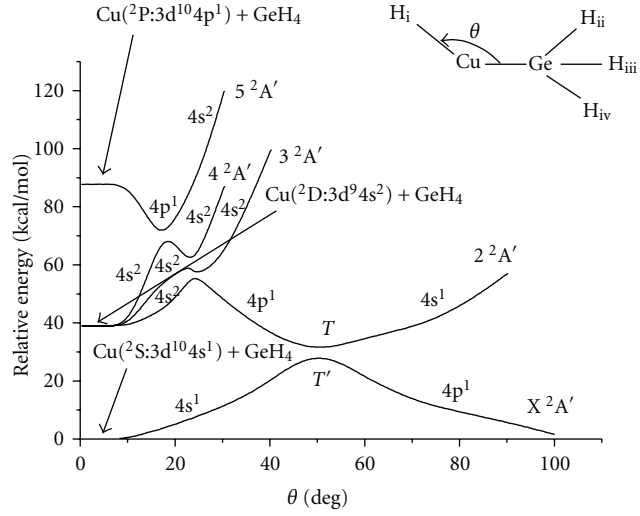

FIGURE 6: Potential energy curves of the Cu(^{2}S, ^{2}D, ^{2}P) interaction with GeH_4 as a function of the insertion angle (θ) towards the $HCuGeH_3$ intermediate product. The $4p^1$ character goes by the path from the second excited state to the minimum in the X ^{2}A′ state, where the final products take place.

Luna-García et al. [12] have found that again copper in its excited state (^{2}P: $3d^{10}$ $4p^1$) breaks a Ge–H bond of germane, overcoming a barrier of 27.0 kcal mol^{-1} of the ground state. The experimental transition energy between the excited state (^{2}P: $3d^{10}$ $4p^1$) and the ground state (^{2}S: $3d^{10}$ $4s^1$) is of 87.8 kcal mol^{-1}, which agrees with the transition energy of 87.7 kcal mol^{-1} theoretically calculated (Table 1). The initial formation of the $HCuGeH_3$ intermediate starts at the minimum (72 kcal mol^{-1}, 17°) with $4p^1$ character and passes through four avoided crossings with the trajectories 4 ^{2}A′, 3 ^{2}A′, 2 ^{2}A′, and X ^{2}A′ of the energy surfaces (see Figure 6). Finally the intermediate with energy 1.6 kcal mol^{-1} (and $4p^1$ character) evolves toward HCu + GeH_3 and $CuGeH_3$ + H products with 27.1 and 33.2 kcal mol^{-1}, respectively (see Table 1). The latter is due to the endergonic nature of the reaction. In the same table, there is only the experimental energy value 21.7 kcal mol^{-1} of HCu + GeH_3 products.

2.2. Interactions of the Zn, Cd, and Hg Pseudotransition Metals with YH_4. Castillo et al. [8] found that Zinc in its first excited state (^{1}P: $3d^{10}$ $4s^1$ $4p^1$) lying 141 kcal mol^{-1} high breaks the C–H bond of methane, while the Zn ground state presents a quite high activation barrier of 90.5 kcal mol^{-1} (see Figure 7, Table 2(a)). The TP of the potential energy surfaces (2 ^{1}A′ → X ^{1}A′) is obtained for the reaction: Zn (^{1}P: $4s^1$ $4p^1$) + CH_4 → Zn (^{1}S: $4s^2$) + CH_4 through one avoided crossing; thenceforth, the products of the reaction Zn + CH_4 are reached. This happens when zinc is photoexcited to the second excited state Zn (^{1}P: $3d^{10}$ $4s^1$ $4p^1$), which allows this zinc atom to be inserted in the methane molecule. The latter effect is initially exhibited at the minimum (93 kcal mol^{-1}, 59°) of the 2 ^{1}A′ state forming the intermediate $HZnCH_3$, which when continuing its path has a probability [82] P = 0.81 of crossing towards the X ^{1}A′ state and a probability

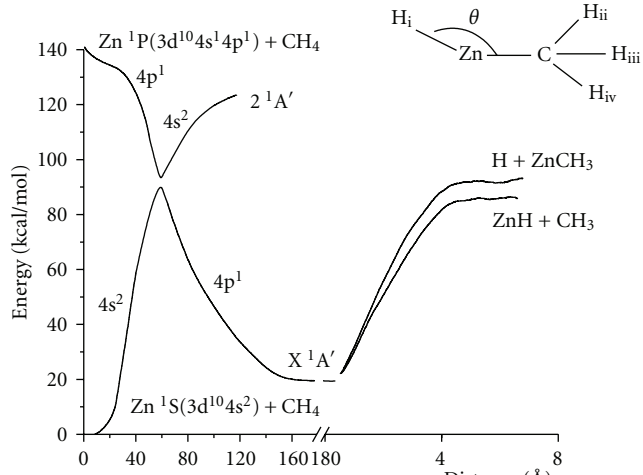

FIGURE 7: Potential energy surfaces of the interaction of both Zn(^{1}S) + CH_4 and Zn(^{1}P) + CH_4. The $4p^1$ character follows the path from the second excited state to the minimum in the X ^{1}A′ state, where the final products are formed. In this figure, Zn… H_i means that product H + ZnCH3 arises from sending to infinity the H_i, and Zn… C means that product ZnH + CH3 arises from sending to infinity the H_iZn.

P = 0.19 of continuing by the same 2 ^{1}A′ state. When following via X ^{1}A′ (see Figure 7), at the minimum of this state, the product formation can be obtained [82]. Finally, acquiring the formation of the $HZnCH_3$ intermediate with a calculated energy of ~25 kcal mol^{-1} that passes through the avoided crossing of 2 ^{1}A′ and X ^{1}A′ sates, with the subsequent formation of HZn + CH_3 and $ZnCH_3$ + H final products,

Table 2

(a) Pseudotransition metal family (Zn, Cd) interacting with methane. Relative energies (kcal mol^{-1}) of the reactants, intermediate $HXCH_3$, and final products for three lowest states of the metals.

M: metal	Zn[a] (^{1}S, ^{3}P, ^{1}P)		Cd[b] (^{1}S, ^{3}P, ^{1}P)	
	ΔE_{Exp}	ΔE_{Cal}	ΔE_{Exp}	ΔE_{Cal}
M(2nd) + CH_4	133.7	~141	124.9	125.6
M(1st) + CH_4	93.4	~94	89.3	84.9
H + MCH_3		~93		67.9
HM + CH_3		~82		56.6
$HMCH_3$		~25		31.9[c]
M(gs) + CH_4	0	0	0	0

[a] From [80]
[b] From [86]
[c] From [95].

(b) Pseudotransition metal family (Zn, Cd, Hg) interacting with silane. Relative energies (kcal mol^{-1}) of the reactants, the $HXSiH_3$ intermediary and final products for threelowest states of these metals.

M: metal	Zn[a] (^{1}S, ^{3}P, ^{1}P)		Cd[b] (^{1}S, ^{3}P, ^{1}P)		Hg[b] (^{1}S, ^{3}P, ^{1}P)	
	ΔE_{Exp}	ΔE_{Cal}	ΔE_{Exp}	ΔE_{Cal}	ΔE_{Exp}	ΔE_{Cal}
M(2nd) + SiH_4	133.7	141	124.9	128.5	154.6	157.6
M(1st) + SiH_4	93.4	93.8	89.3	84.4	119.5	114.6
H + $MSiH_3$		84		89.0		95.4
HM + SiH_3	70.4	74	74	75.5	83.33	87.6
$HMSiH_3$		11.5		20.7		28.0
M(gs) + SiH_4	0	0	0	0	0	0

[a] From [9]
[b] From [10].

(c) Pseudotransition metal family (Cd, Hg) interacting with germane. Relative energies (kcal mol^{-1}) of the reactants, the $HXGeH_3$ intermediary, and final products for three lowest states of these metals.

X: metal	Cd[a] (^{1}S, ^{3}P, ^{1}P)		Hg[a] (^{1}S, ^{3}P, ^{1}P)	
	ΔExp[b]	ΔE_{Cal}	ΔExp[b]	ΔE_{Cal}
X(2nd) + GeH_4	124.9	128.5	154.6	157.6
X(1st) + GeH_4	89.3	84.4	119.5	114.6
H + $XGeH_3$		79.9		87.7
HX + GeH_3	68.9	70.3	75.3	80.0
$HXGeH_3$		13.6		21.0
X(gs) + GeH_4	0	0	0	0

[a] From [10]
[b] From [93].

with the corresponding energies ~82 and ~93, respectively; as it can be seen in Table 2(a).

Ramírez-Solís and Castillo [86] compared the C_{3v} versus C_{2v} symmetries of Cd (^{1}S, ^{3}P, ^{1}P) + CH_4 interactions in the edge on geometry orientation. For C_{3v} symmetry, they calculated two more geometry orientations. Before starting their molecular calculations, they successfully reproduced the lowest states of the atomic spectra of cadmium as mentioned in Table 2(a) which corresponds to 125.6 kcal mol^{-1} for the second excited state. They did not construct the potential energy surfaces; however, they calculated the breaking of the C–H bond of methane with the consequent formation of an intermediate with energy of 31.9 kcal mol^{-1} and its decomposition in possible products: HCd + CH_3 and H + $CdCH_3$ with energy of 56.6 and 67.9 kcal mol^{-1}, respectively (see Table 2(a)).

Luna-García et al. [9] found that Zinc in its singlet second excited state (^{1}P: $3d^{10}$ $4s^1$ $4p^1$) breaks the Si–H bond of silane, by reversing the initially repulsive ground state curve, thus, overcoming a barrier of ~80 kcal mol^{-1} of the latter. The experimental transition energy between the excited state (^{1}P: $3d^{10}$ $4s^1$ $4p^1$) and the singlet ground state (^{1}S: $3d^{10}$ $4s^2$) is 133.7 kcal mol^{-1}, which is comparable to the calculated transition energy of 141.0 kcal mol^{-1} of the second excited

state of Zinc calculated theoretically (Table 2(b), Figure 8). The formation of the $HZnSiH_3$ intermediate arising at the minimum (81 kcal mol^{-1}, 60°) comes with $4p^1$ character and approaches the avoided crossing between $2\,^1A'$ and $X\,^1A'$ states keeping $4p^1$ character until the end of the latter state with an energy 11.5 kcal mol^{-1}. Finally, due to the endergonic nature of this reaction, the intermediate leads toward the HZn + SiH_3 and $ZnSiH_3$ + H products with calculated energies of 74.0 and 84.0 kcal mol^{-1}, respectively (see Table 2(b)). The experimental energy for HZn + SiH_3 products is 70.4 kcal mol^{-1} in agreement with that calculated theoretically. We have not calculated transition probabilities yet.

Luna-García et al. [10] found that cadmium in its singlet second excited state (^{1}P: $4d^{10}\ 5s^1\ 5p^1$) breaks the Si–H bond of silane, creating a barrier of ∼89 kcal mol^{-1} for the ground state. The experimental transition energy between the excited state (^{1}P: $4d^{10}\ 5s^1\ 5p^1$) and the ground state (^{1}S: $4d^{10}\ 5s^2$) is 124.9 kcal mol^{-1}, which is comparable to the transition energy of 128.5 kcal mol^{-1} calculated theoretically (Table 2(b), Figure 9). The formation of the $HCdSiH_3$ intermediate at the minimum (92 kcal mol^{-1}, 45°) comes with $5p^1$ character, passes through the avoided crossing between $2\,^1A'$ and $X\,^1A'$ pathways, and keeps $5p^1$ character until the minimum (20.7 kcal mol^{-1}, 180°) of the $X\,^1A'$ state is reached (see Figure 9). Finally, the intermediate is broken reaching the HCd + SiH_3 and $CdSiH_3$ + H products with calculated energies of 75.5 and 89 kcal mol^{-1}, respectively (see Table 2(b)). The experimental energy for HCd + SiH_3 is 74.0 kcal mol^{-1}. We have not calculated transition probabilities yet.

Luna-García et al. [9] found that mercury in its singlet second excited state (^{1}P: $5d^{10}\ 6s^1\ 6p^1$) breaks the Si–H bond of silane, leading to a ground state barrier of ∼102 kcal mol^{-1}. The experimental transition energy between the excited state (^{1}P: $5d^{10}\ 6s^1\ 6p^1$) and the singlet ground state (^{1}S: $5d^{10}\ 6s^2$) is 154.6 kcal mol^{-1}, which agrees to the transition energy of 157.6 kcal mol^{-1} theoretically calculated (see Figure 10 and Table 2(b)). The formation of the $HHgSiH_3$ intermediate arising at the minimum (106 kcal mol^{-1}, 70°) comes with $6p^1$ character and passes through an avoided crossing between trajectories $2\,^1A'$ and $X\,^1A'$ of the energy surfaces maintaining $6p^1$ character. The transition probability [84] at the avoided crossing among the latter states is obtained when mercury is photoexcited to the Hg ^{1}P: $5d^{10}\ 6s^1\ 6p^1$ excited state, allowing it to be inserted in silane (SiH_4) molecule. When the reaction pathway passes the crossing point and continues its way has a probability $P = 0.79$ of crossing toward curve $X\,^1A$ with $6p^1$ character and a probability of $P = 0.21$ of continuing in the same curve $2\,^1A'$ (see Figure 10) with $6s^2$ character. When going toward the $X\,^1A'$ state, it allows the formation of a stable intermediate at the minimum (28 kcal mol^{-1}, 180°) of the state. Finally, the latter is broken and reaches either the HHg + SiH_3 or $HgSiH_3$ + H products with energies 87.6 and 95.4 kcal mol^{-1}, respectively.

Luna-García et al. [11] have found that Cadmium in its singlet second excited state (^{1}P: $4d^{10}\ 5s^1\ 5p^1$) breaks the Ge–H bond of germane, while producing a ground state

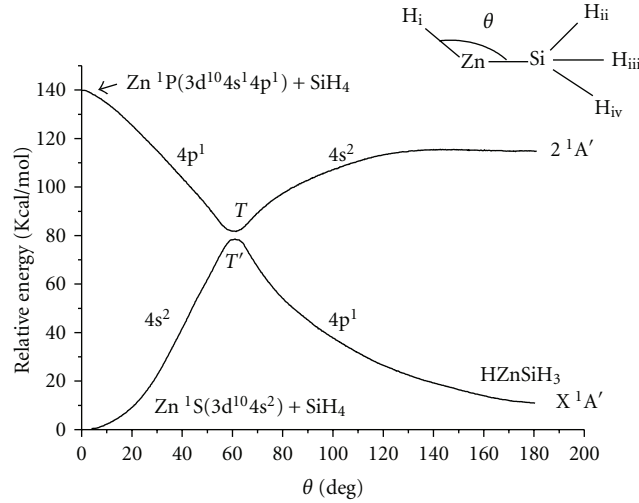

FIGURE 8: Potential energy curves of the Zn(^{1}S, ^{1}P) interaction with SiH_4 as a function of the insertion angle (θ) towards the $HZnSiH_3$ intermediate product. The 4p1 character follows the path from the second excited state to the minimum in the X ^{1}A′ state, where the final products are formed.

barrier of 83.6 kcal mol^{-1} (see Figure 11). The experimental transition energy between the excited state (^{1}P: $4d^{10}\ 5s^1\ 5p^1$) and the ground state (^{1}S: $4d^{10}\ 5s^2$) is 124.9 kcal mol^{-1}, which agrees with the transition energy of 128.5 kcal mol^{-1} calculated theoretically (Table 2(c)). The formation of the $HCdGeH_3$ intermediate at (89 kcal mol^{-1}, 50°) comes with $5p^1$ character and goes by an avoided crossing between the $2\,^1A'$ and $X\,^1A'$ states maintaining a $5p^1$ character until the next minimum at (13.6 kcal mol^{-1}, 180°) (see Figure 11). Finally the intermediate is broken in the HCd + GeH_3 and $CdGeH_3$ + H products with calculated energies 70.3 and 79.9 kcal mol^{-1}, respectively. The experimental energy for HCd + GeH_3 is 68.9 kcal mol^{-1}. We have not calculated the transition probabilities yet.

Luna-García et al. [11] have found that mercury in its excited state (^{1}P: $5d^{10}\ 6s^1\ 6p^1$) breaks the Ge–H bond of germane, while forming a ground state barrier of 86.1 kcal mol^{-1}. The experimental transition energy between the excited state (^{1}P: $5d^{10}\ 6s^1\ 6p^1$) and the ground state (^{1}S: $5d^{10}\ 6s^2$) amounts to 154.6 kcal mol^{-1}, in good agreement with the transition energy of 157.6 kcal mol^{-1} theoretically calculated (Table 2(c)). The transition probability [84] between the PES is obtained for the reaction Hg ^{1}P($5d^{10}\ 6s^1\ 6p^1$) + GeH_4 → Hg ^{1}S($5d^{10}\ 6s^2$) + GeH_4. When mercury is photoexcited to the Hg (^{1}P:$5d^{10}\ 6s^1\ 6p^1$) second excited state, the mercury atom is inserted in germane (GeH_4) molecule. This effect is observed in the minimum (90 kcal mol^{-1}, 60°) of the $2\,^1A'$ state arriving with $6p^1$ character, where the $HHgGeH_3$ intermediate is formed. When this intermediate continues its way, it has a probability $P = 0.83$ of crossing toward $X\,^1A$ state with $6p^1$ character and a probability of $P = 0.17$ of continuing in the same $2\,^1A'$ state (see Figure 12) with $6s^2$ character. When going toward the $X\,^1A'$ state, it leads to the formation of the product at the minimum

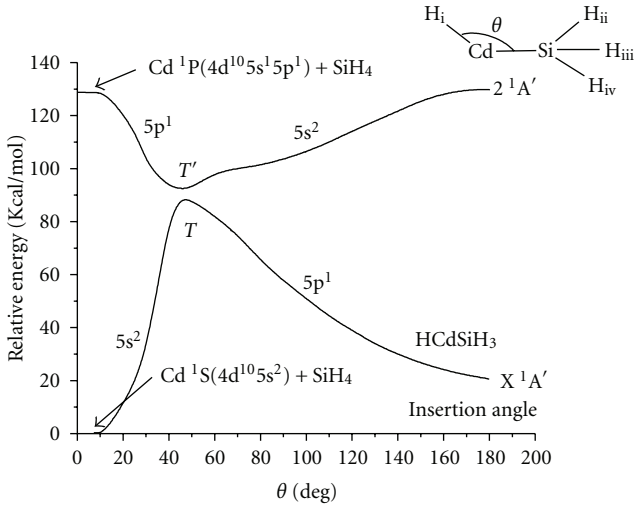

Figure 9: Potential energy curves of the Cd(^{1}S, ^{1}P) interaction with SiH_4 as a function of the insertion angle (θ) towards the $HCdSiH_3$ intermediate product. The $5p^1$ character follows the path from the second excited state to the minimum in the X ^{1}A′ state, where the final products are formed.

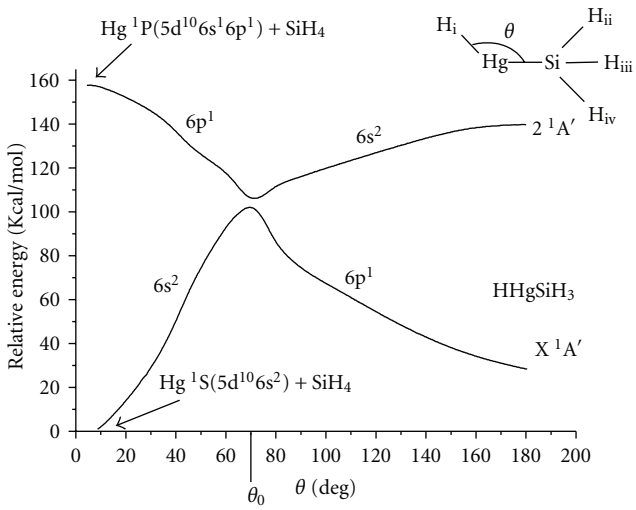

Figure 10: Potential energy curves of the Hg(^{1}S, ^{1}P) interaction with SiH_4 as a function of the insertion angle (θ) towards the $HHgSiH_3$ intermediate product. The $6p_1$ character follows the path from the second excited state to the minimum in the X ^{1}A′ state, where the final products are formed.

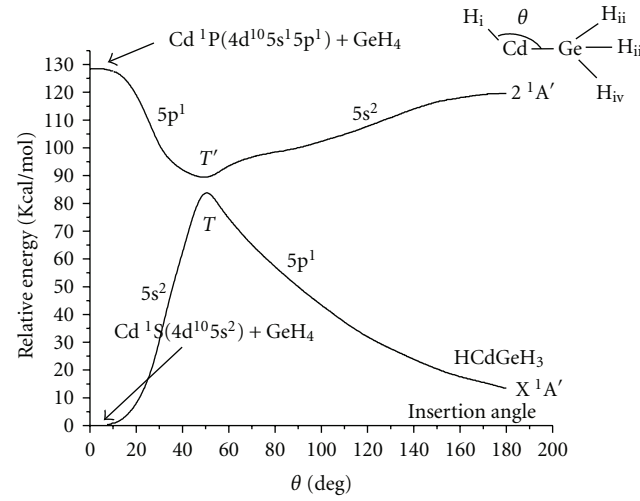

Figure 11: Potential energy curves of the Cd(^{1}S, ^{1}P) interaction with GeH_4 as a function of the insertion angle (θ) towards the $HCdGeH_3$ intermediate product. The $5p^1$ character follows the path from the second excited state to the minimum in the X ^{1}A′ state, where the final products are formed.

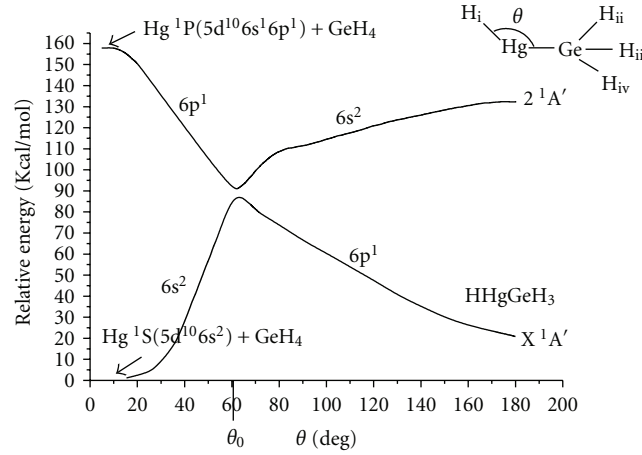

Figure 12: Potential energy curves of the Hg(^{1}S, ^{1}P) interaction with GeH_4 as a function of the insertion angle (θ) towards the $HHgGeH_3$ intermediate product. The$6p^1$ character followed the path from the second excited state to the minimum in the X ^{1}A′ state, where the final products are formed.

(21 kcal mol^{-1}, 180°) of the state. Finally, the intermediate evolves towards the HHg + GeH_3 and $HgGeH_3$ + H products with calculated energies 80 and 87.7 kcal mol^{-1}, respectively, while the experimental energy for HHg + GeH_3 is 75.3 kcal mol^{-1}.

2.3. Interactions of the Al, Ga Metals with YH_4. Pacheco-Blas et al. [88] found that the aluminum in its doublet second excited state (^{2}D: $3s^2$ $3d^1$) breaks the C–H bond of methane, as does the 2 ^{2}A′ state after surpassing an activation barrier of 14.0 kcal mol^{-1} (see Figure 13). The experimental transition energy between this second excited state (^{2}D: $3s^2$ $3d^1$) and the ground state (^{2}P: $3s^2$ $3p^1$) is 92.5 kcal mol^{-1} and agrees with the transition energy of 93.9 kcal mol^{-1} theoretically calculated (see Table 3(a)). The transition probability [88] among the corresponding PES for the reaction Al ^{2}D($3s^2$ $3d^1$) + CH_4 → Al ^{2}P($3s^2$ $3p^1$) + CH_4 starts with the formation of the $HAlCH_3$ intermediate and goes through two avoided crossings with the 3 ^{2}A′, 2 ^{2}A′, and X ^{2}A′ states. When aluminum is photoexcited to its Al ^{2}D: $3s^2$ $3d^1$ second excited state, it is inserted into a C–H bond of methane at the minimum (87 kcal mol^{-1}, 20°) in the 3 ^{2}A′ state with $3d^1$ character. Under these conditions, the $HAlCH_3$ intermediate is formed. As the latter continues its path, it

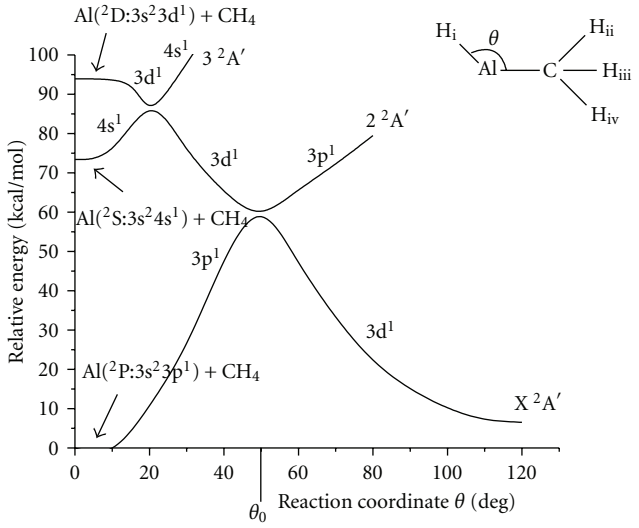

FIGURE 13: Potential energy curves of the Al (^{2}P, ^{2}S, and ^{2}D) interaction with CH_4 versus θ insertion angle toward the $HAlCH_3$ intermediate product. The $3d^1$ character follows the path from the second excited state to the minimum in the X ^{2}A′ state, where the final products are formed.

has a probability of 0.85 of crossing toward the 2 ^{2}A′ state with $3d^1$ character going to the Al ^{2}D: $3s^2$ $4s^1$ first state and a probability of 0.15 of continuing in the same 3 ^{2}A′ state with $4s^1$ character. When the intermediate continues its pathway, there is a probability of 0.89 for crossing from the 2 ^{2}A′ state to the X ^{2}A′ with $3d^1$ character (see Figure 13), where the most stable intermediate is found at $\theta = 120°$ and 6.5 kcal mol^{-1}. When this occurs, the final products are reached from the Al + CH_4 reaction, that is, to say, the intermediate is broken in the HAl + CH_3 and $AlCH_3$ + H products with calculated energies 42.8 and 48.2 kcal mol^{-1}, respectively. In this case, the corresponding experimental [36] energy is 45.0 kcal mol^{-1} in both cases.

Pacheco-Sánchez et al. [14] have found that gallium in its doublet first excited state (^{2}S: $4s^2$ $5s^1$) breaks the C–H bond of methane, producing in the lowest state an activation barrier of 53.7 kcal mol^{-1}. The experimental transition energy among the excited state (^{2}S: $4s^2$ $5s^1$) and the ground state (^{2}P: $4s^2$ $4p^1$) is 69.3 kcal mol^{-1}, in agreement with the transition energy 72.7 kcal mol^{-1} theoretically calculated (see Table 3(a)), within the 3 kcal mol^{-1} of tolerance. The transition probability [14] among the corresponding PES for the reaction Ga ^{2}S($4s^2$ $5s^1$) + CH_4 → Ga ^{2}P($4s^2$ $4p^1$) + CH_4 starts with the formation of the intermediate $HGaCH_3$ and passes through two avoided crossings with 3 ^{2}A′, 2 ^{2}A′, and X ^{2}A′ states. When gallium is photoexcited to its Ga ^{2}S: $4s^2$ $5s^1$ first excited state, it is inserted into a C–H bond of methane at the minimum (60 kcal mol^{-1}, 25°) in the 3 ^{2}A′ state with $5s^1$ character. Under these conditions, the intermediate product $HGaCH_3$ is formed. As the latter continues its path, it has a probability of 0.715 [83] (the branching fraction is 0.73 [96]) of crossing toward the 2 ^{2}A′ state with $5s^1$ character going to the Ga ^{2}P: $4s^2$ $4p^1$ ground state and a probability of 0.285 of continuing by the same 3 ^{2}A′ state with $4p^1$ character. When the intermediate continues its pathway, there is a probability of 0.46 for crossing from the 2 ^{2}A′ state to X^{2}A′ with $5s^1$ character (see Figure 14), where the most stable intermediate is found at $\theta = 120°$ and 6.1 kcal mol^{-1}. Finally, this intermediate is broken in the products HGa + CH_3 and $GaCH_3$ + H with calculated energies 40.2 and 45.7 kcal mol^{-1}, respectively. The corresponding experimental energy is 38.9 kcal mol^{-1} in HGa + CH_3 case.

Pacheco-Sánchez et al. [13] have found that gallium in its doublet first excited state (^{2}S: $4s^2$ $5s^1$) breaks the Si–H bond of silane, overcoming a barrier of 51.0 kcal mol^{-1} of the ground state. The experimental transition energy between the excited state (^{2}S: $4s^2$ $5s^1$) and the ground state (^{2}P:$4s^2$ $4p^1$) is 69.3 kcal mol^{-1}, which agrees to the transition energy of 71.7 kcal mol^{-1} theoretically calculated (Table 3(b)). The transition probability [13] among the corresponding PES for the reaction Ga ^{2}S($4s^2$ $5s^1$) + SiH_4 → Ga ^{2}P($4s^2$ $4p^1$) + SiH_4 starts with the formation of the intermediary molecule $HGaSiH_3$ passing through two avoided crossings among 3 ^{2}A′, 2 ^{2}A′, and X ^{2}A′ states. The probability [85] that it crosses from 3 ^{2}A′ state to 2 ^{2}A′ state is $P = 0.701$ and a probability $P = 0.299$ of continuing along the same 3 ^{2}A′ state. When crossing towards the 2 ^{2}A′ state in its descent, it has a probability $P = 0.685$ of crossing towards the X ^{2}A′ state and a probability $P = 0.315$ of continuing along the same 2 ^{2}A′ state (see Figure 15). Finally at the minimum (6.1 kcal mol^{-1}, 120°) of the X ^{2}A′ state, the intermediate is broken into the HGa + SiH_3 and $GaSiH_3$ + H products with energies 26.1 and 45.3 kcal mol^{-1}, respectively. The corresponding experimental energy is 24.5 kcal mol^{-1} in HGa + SiH_3 case.

Lefcourt and Ozin [100] optimized geometry of Al–SiH_4 interaction for $^2A_1$ state in C_{2v} symmetry with the single point SCF energy and calculated that the geometry-optimized structure does not differ very much at all from the initial geometry, a situation that is reflected in the converged energy which is only approximately 1/100 of a hartree lower (~6.21 kcal/mol) than the single-point value associated with the starting structure. Calculations carried out on systems having the equivalent starting geometry but inhabiting the $^2B_1$ and $^2B_2$ electronic states yielded final energies that were considerably higher (0.17 and 0.31 hartree, resp.) than the energy obtained in the $^2A_1$ optimization.

3. Discussion

We have presented here a series of studies on X + YCH_4 (X = Cu, Zn, Cd, Ga, Al, Au, Hg, and Y = C, Si, Ge) reactions, attempting to identify possible general patterns. The very first study presented, the Cu + CH_4 reaction was simultaneously being studied experimentally at Toronto University in Canada [32, 33, 101–104], allowing us to make a very close comparison and correlation between their cryogenic experiments and our quantum mechanical calculations. This was due to the fact that Jaime Garcia-Prieto (a member of our group in Mexico) was working with Professor Geoffrey Ozin at Lash Miller Lab. in Toronto

Table 3

(a) Metal family (Al, Ga) interacting with methane. Relative energies (kcal mol^{-1}) of the reactants, intermediary $HXCH_3$ and final products for three lowest states of the metal.

X: metal	Al[a] (^{2}P, ^{2}S, ^{2}D)		Ga[b] (^{2}P, ^{2}S, ^{2}P)	
	ΔE_{Exp}	ΔE_{Cal}	ΔE_{Exp}	ΔE_{Cal}
X(2nd) + CH_4	92.5	93.9	93.1	93.7
X(1st) + CH_4	72.24	73.4	69.3	72.7
H + XCH_3	45.0	48.2		45.7
HX + CH_3	45.0	42.8	38.9[c]	40.2
$HXCH_3$	⋯	6.5	4.9[d]	6.1
X(gs) + CH_4	0	0	0	0

[a]From [88]
[b]From [14]
[c]From [97]
[d]From [98].

(b) Metal family (Al, Ga) interacting with silane. Relative energies (kcal mol^{-1}) of the reactants, the $HXSiH_3$ intermediary and final products for three lowest states of the metals.

X: metal	Al[a] (^{2}P, ^{2}S, ^{2}D)		Ga[b] (^{2}P, ^{2}S, ^{2}P)	
	ΔE_{Exp}	ΔE_{Cal}	ΔE_{Exp}	ΔE_{Cal}
X(2nd) + SiH_4	92.5		93.1	93.7
X(1st) + SiH_4	72.24		69.3	71.7
H + $XSiH_3$				45.3
HX + SiH_3			24.5[c]	26.1
$HXSiH_3$		6.21[d]		6.1
X(gs) + SiH_4	0	0	0	0

[a]From [88]
[b]From [13]
[c]From [97]
[d]From [99].

on the photochemical activation of Cu in methane matrices at near-absolute zero conditions. Originally Ozin expected the open shell Cu: ^{2}D excited state to be responsible for methane activation, but our calculations proved that the higher lying ^{2}P was the real culprit, albeit through a series of avoided crossings a fact which was finally acknowledged in the experimental and theoretical papers [32, 60]. Since then our group, mainly through the late Sidonio Castillo and his collaborators, studied a series of transition metals. We have presented here an overview of this line of research although we evidently must accept that the list of metals studied to date is far from exhaustive. This notwithstanding, we provide here enough examples of the mechanism first advanced in our explanation of the Lash Miller Lab experiments of the activation of methane by copper [60, 82]. In short we have advanced a daring hypothesis avoided crossings and transition probabilities for curves of the same symmetry play a systematic and clear-cut role in the activation of methane, silane, and germane. Indeed, we show the evidence that in general, the most stable intermediate has a rather weak binding, thus leading to the products. The potential energy surfaces lead from the reactants climbing to this transition state which requires moderate energies, normally derived from photoactivation processes and finally yielding the final products (XH + YH_3 or H + XYH_3). To document this, we report the configurations and bond distances as they evolve in each specific case. We kindly refer our readers to access our original papers for details. In any case, our reported energies are compatible with the spectra of reactants, intermediates, and products. For instance, the probabilities for the Ga + CH_4 reaction agree quite well with experimental results [83, 96], whereas those obtained for other systems reported here were widely discussed in the original papers [82–88].

The potential energy surfaces for the coinage metals Cu and Au with silane are rather similar. The main difference lies in the energies of their respective second excited states, making their potential energy wells differ from their respective intermediate complexes onward to the final products. To wit, in the Au + SiH_4 reaction, the minimum at 120 degrees has only a depth of 3.34 kcal/mol, while for Cu + SiH_4 the minimum lies at 100 degrees and is 5.58 kcal/mol deep. These results would make the study of the Ag + SiH_4 reaction all the more desirable, a valid proposition for several other metals. We explicitly state here that our work on these systems is far from complete. Take for instance our results involving Hg which are rather different from

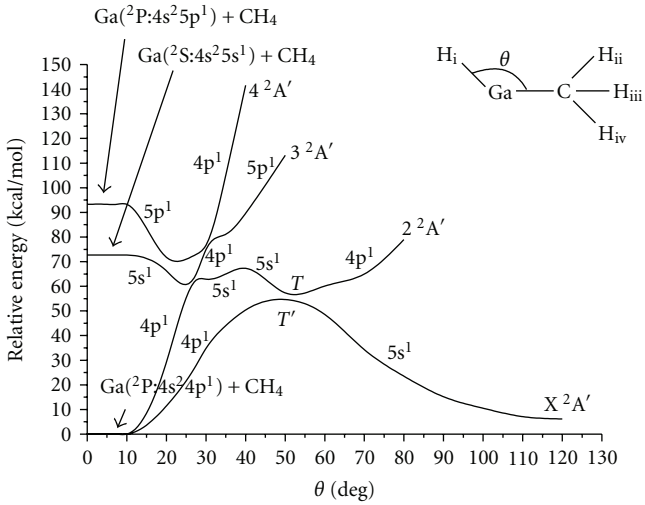

Figure 14: Potential energy curves of the interaction of Ga(^{2}P), Ga(^{2}S), and Ga(^{2}P) with CH_4 towards the $GaCH_3$ intermediate. Energy versus insertion angle (θ). The $5s^1$ character follows the path from the first excited state to the minimum in the X ^{2}A′ state, where the final products emerge.

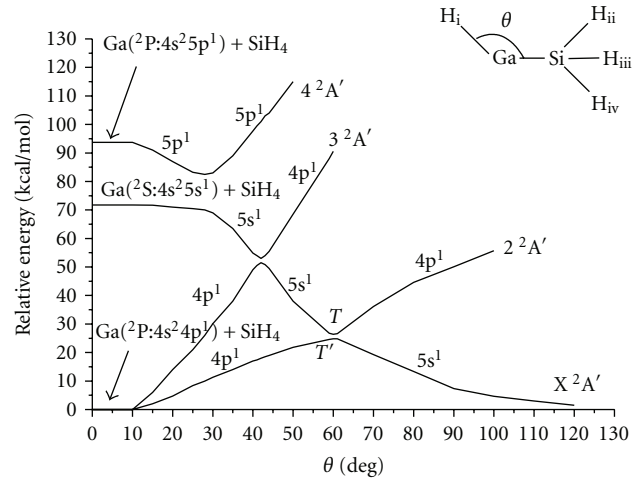

Figure 15: Potential energy curves of the interaction of Ga(^{2}P), Ga(^{2}S), and Ga(^{2}P) with SiH_4 towards the $GaSiH_3$ intermediate. Energy versus insertion angle (θ). The $5s^1$ character followed the path from the first excited state to the minimum in the X ^{2}A′ state, where the final products are formed.

the other metals, thus, naturally deserving closer scrutiny. Perhaps we may tentatively relate this peculiarity of mercury to its particularly stable ground state $^1S_0$ (with its closed $5d^{10}$ $6s^2$ valence shell), from which stem the unique dense metal liquid character of mercury, in dire contrast with its solid metal neighbors with stable electronic arrangements. In effect we dare propose that this line of research is both valid and promising and needs much more work and attention, especially so with a close collaboration with cryogenic experiments, as we hope to establish.

Difference of PES of coinage metals interacting with silane is due to the second excited state leading to the reported well depths for the potentials for the ground state. Analogously, the PES of pseudotransition metals interacting with silane is very similar, and the main difference is the ^{1}P singlet energy of the pseudotransition metals at the second excited state. This causes the depth wells of potential (11.5 kcal mol^{-1}, 180°) for Zn + SiH_4, while for Cd + SiH_4 it is (20.7 kcal mol^{-1}, 180°), and for Hg it is (28 kcal mol^{-1}, 180°), since the initial formation of the intermediate until the product formation.

The methane complexes with Zn and Cd in the second excited state ^{1}P at $\theta = 0$ has energies ∼141 and 125.6 kcal mol^{-1}, respectively. The germane complexes with Cd and Hg in the second excited state ^{1}P at $\theta = 0$ have energies 128.5 and 157.6 kcal mol^{-1}, respectively. The initial excitation energy of the pseudotransition metals yields the depth wells of potential, which is ∼25 kcal mol^{-1} for Zn + CH_4 and 31.9 kcal mol^{-1} Cd + CH_4. The initial excitation energy of the pseudotransition metals yields the depth wells of potential, which is 13.6 and 21.0 kcal mol^{-1} for Cd + GeH_4 and Hg + GeH_4, respectively.

Finally, PES of metals Al ^{2}D doublet and Ga ^{2}P doublet in the second excited state interacting with methane for $\theta = 0$ has energies 93.9 and 93.7 kcal mol^{-1}, respectively. The initial energy of the metals yields the depth wells of potential, of 6.5 and 6.1 kcal mol^{-1} for Al + CH_4 and Ga + CH_4, respectively, and 6.21 taken from reference [100] and 6.1 kcal mol^{-1} for Al + SiH_4 and Ga + SiH_4, respectively. While the latter result is as expected, in the previous one there is a very small deviation. This is due to the very small energy difference at 2nd excited state between Al and Ga, and to the approximation error carried out by the numerical solutions of the system. In defense of this argumentation, it is the fact that the dissociation energy of the ionic Al^+-CH_4 complex has been experimentally reported to be 2120 ± 105 cm^1 (6.06 ± 0.3 kcal mol^{-1}) [99]. Somewhat coincidentally we have obtained the value of 6.5 kcal mol^{-1} for the dissociation energy of Al + CH_4 complex. It is quite remarkable that the dissociation energies for Al^+-CH_4 and Al + CH_4 are quite close, and that the experimental value for this ionic Al^+–CH_4 reaction is the expected value for the dissociation energy of Al–CH_4.

A very important issue is to get the most stable intermediate with the lowest energy on which the breaking of the intermediate is achieved. The products of the reaction emerge at the end from the X A′ state, calculated using the parameter values obtained at this minimum.

The intermediate has a much lower energy than the final products due to the endergonic nature of these reactions. Initially, the metal needs a photoexcitation for taking it to an excited state for being inserted in a Y–H bond of the gas molecule, in order to surpass the activation barrier of the ground state for the reaction. After the avoided crossings, the deformed metastable intermediate arrives to the most stable arrangement, having the lowest energy with the optimal geometry. At this low energy arrangement, its internal bond orientation produces a still strong electrostatic repulsion due to the energy gained by the photoexcitation of the metal, greater than the energy of the intermediate. The metal atom

also shares its energy with the carbon and hydrogens. Thus, the new energies of the products cannot be greater than the initial excitation of the metal or lower than the energy of the reactants in their ground state.

The resulting probabilities for the case of Ga + CH_4 are in agreement with previous experimental results [83], whereas those obtained for the other cases are only theoretical predictions.

4. Conclusions

From the theory of transition probabilities at avoided crossings between curves of the same symmetry, we can deduce that the character of the wave function is the same at the beginning of the highest state path than at the minimum of the ground state path after all avoided crossings.

The energy value of the initial state of the metal which eventually leads to the intermediate, as well as the character of the wavefunction is crucial for the product formation. This character corresponds to the dominant excited state of the metal inserting in the gas molecule and is independent of the gas in consideration (methane, silane, or germane).

As expected the wells' potential depth is dependent on the energy level of the metal excited state in consideration, and the pathway is reflected in the character of the wavefunction revealing the electronic configuration of the corresponding excited state. This means that the higher the energy of the metal atom excited state, the deeper the potential energy well at the ground state minimum.

References

[1] J. P. Daudey, PSHF, a HF-SCF RECP program, based on the original HONDO-76, QCPE program no. 338 by M Dupuis, J. Rys, H. F. King, 1977.

[2] P. H. Durand and J. C. Barthelat, "A theoretical method to determine atomic pseudopotentials for electronic structure calculations of molecules and solids," *Theoretica Chimica Acta*, vol. 38, no. 4, pp. 283–302, 1975.

[3] J. C. Barthelat, P. H. Durand, and A. Serafini, "Non-empirical pseudopotentials for molecular calculations," *Molecular Physics*, vol. 33, no. 1, pp. 159–180, 1977.

[4] J. C. Barthelat, P. H. Durand, A. Serafini et al., "Recent progress of pseudopotentials in quantum chemistry," *Gazzetta Chimica Italiana*, vol. 108, p. 225, 1978.

[5] M. Pelissier and P. Durand, "Testing the arbitrariness and limits of a pseudopotential technique through calculations on the series of diatoms HF, AlH, HCl, AlF, AlCl, F2, Cl2," *Theoretica Chimica Acta*, vol. 55, no. 1, pp. 43–54, 1980.

[6] R. Carbó, M. Pélissier, J. P. Daudey, and J. Rubio, *GMCP Program Based on the Elementary Jacobi Rotation Algorithm*, 1993.

[7] B. H. Huron, J. P. Malrieu, and P. Rancurel, "Iterative perturbation calculations of excited ground and excited state energies from multiconfigurational zeroth-order wavefunctions," *Journal of Chemical Physics*, vol. 58, pp. 5745–5759, 1973, CIPSI code written by J. P. Daudey, M Pélissier, J. P. Malrieu, S. Evangelisti, F. Spiegelmann, and D. Maynau.

[8] S. Castillo, A. Ramírez-Solís, D. Díaz, E. Poulain, and O. Novaro, "Theoretical study of the activation of methane by photoexcited zinc atoms," *Molecular Physics*, vol. 81, no. 4, pp. 825–836, 1994.

[9] H. Luna-García, S. Castillo, and A. Ramírez-Solís, "Ab initio study of the reactions of Zn(^{1}S, ^{3}P, and ^{1}P) with SiH4," *Journal of Chemical Physics*, vol. 107, no. 17, pp. 6627–6633, 1997.

[10] H. Luna-García, S. Castillo, and A. Ramírez-Solís, "Ab initio studies of the reactions of M(^{1}S, ^{3}P, and ^{1}P) with SiH4 (M = Cd, Hg)," *Journal of Chemical Physics*, vol. 110, no. 23, pp. 11315–11322, 1999.

[11] H. Luna-García, S. Castillo, and A. Ramírez-Solís, "Ab initio studies of the reactions of M(^{1}S, ^{3}P, and ^{1}P) with GeH4 (M = Cd, Hg)," *Journal of Chemical Physics*, vol. 114, no. 6, pp. 2647–2652, 2001.

[12] H. Luna-García, A. Ramírez-Solís, and S. Castillo, "Ab initio studies of the reactions of Cu(^{2}S, ^{2}D, and ^{2}P) with SiH_4 and GeH_4," *Journal of Chemical Physics*, vol. 116, no. 3, pp. 928–935, 2002.

[13] J. H. Pacheco-Sánchez, H. Luna-García, and S. Castillo, "Ab initio study of the reactions of Ga(^{2}P, ^{2}S, and ^{2}P) with silane," *Journal of Chemical Physics*, vol. 121, no. 12, pp. 5777–5782, 2004.

[14] J. H. Pacheco-Sánchez, H. Luna-García, and S. Castillo, "Ab initio study of the reactions of Ga(^{2}P, ^{2}S, and ^{2}P) with methane," *Journal of Chemical Physics*, vol. 120, no. 9, pp. 4240–4246, 2004.

[15] P. Chaquin, A. Papakondylis, C. Giessner-Prettre, and A. Sevin, "Theoretical study of the quenching of the low-lying excited states of lithium and magnesium by methane," *Journal of Physical Chemistry*, vol. 94, no. 19, pp. 7352–7357, 1990.

[16] L. D. Landau, "Theory of energy transfer II," *Physikalische Zeitschrift der Sowjetunion*, vol. 2, pp. 46–51, 1932.

[17] C. Zener, "Non-adiabatic crossing of energy levels," *Proceedings of the Royal Society A*, vol. 137, no. 833, pp. 696–702, 1932.

[18] R. Robertson and A. Gallagher, "Mono- and disilicon radicals in silane and silane-argon dc discharges," *Journal of Applied Physics*, vol. 59, no. 10, pp. 3402–3411, 1986.

[19] W. M. M. Kessels, A. Leroux, M. G. H. Boogaarts, J. P. M. Hoefnagels, M. C. M. van de Sanden, and D. C. Schram, "Cavity ring down detection of SiH3 in a remote SiH4 plasma and comparison with model calculations and mass spectrometry," *Journal of Vacuum Science and Technology A*, vol. 19, no. 2, pp. 467–476, 2001.

[20] R. Nozawa, H. Takeda, M. Ito, M. Hori, and T. Goto, "In situ observation of hydrogenated amorphous silicon surfaces in electron cyclotron resonance hydrogen plasma annealing," *Journal of Applied Physics*, vol. 85, no. 2, pp. 1172–1177, 1999.

[21] M. Abe, T. Nakajima, and K. Hirao, "A theoretical study of the low-lying states of the AuSi molecule: an assignment of the excited A and D states," *Journal of Chemical Physics*, vol. 117, no. 17, pp. 7960–7967, 2002.

[22] N. Toshima, "Core/shell-structured bimetallic nanocluster catalysts for visible-light-induced electron transfer," *Pure and Applied Chemistry*, vol. 72, no. 1-2, pp. 317–325, 2000.

[23] J. Westwater, D. P. Gosain, K. Yamauchi, and S. Usui, "Nanoscale silicon whiskers formed by silane/gold reaction at 335 °C," *Materials Letters*, vol. 24, no. 1–3, pp. 109–112, 1995.

[24] G. E. Moore, "Cramming more components onto integrated circuits," *Electronics*, vol. 38, no. 8, pp. 114–117, 1965.

[25] R. Solanki, J. Huo, J. L. Freeouf, and B. Miner, "Atomic layer deposition of ZnSe/CdSe superlattice nanowires," *Applied Physics Letters*, vol. 81, no. 20, pp. 3864–3866, 2002.

[26] J. Westwater, D. P. Gosain, S. Tomiya, S. Usui, and H. Ruda, "Growth of silicon nanowires via gold/silane vapor-liquid-solid reaction," *Journal of Vacuum Science and Technology B*, vol. 15, no. 3, pp. 554–557, 1997.

[27] K. Shintani and S. Kameoka, "Molecular-dynamics modelling of the tensile deformation of helical nanowires U6.12.1," in *Materials Research Society Symposium Proceedings*, vol. 778, 2003.

[28] L. Guczi, G. Petö, A. Beck et al., "Gold nanoparticles deposited on SiO_2/Si(100): correlation between size, electron structure, and activity in CO oxidation," *Journal of the American Chemical Society*, vol. 125, no. 14, pp. 4332–4337, 2003.

[29] J. Guzman and B. C. Gates, "Catalysis by supported gold: correlation between catalytic activity for CO oxidation and oxidation states of gold," *Journal of the American Chemical Society*, vol. 126, no. 9, pp. 2672–2673, 2004.

[30] M. Valden, X. Lai, and D. W. Goodman, "Onset of catalytic activity of gold clusters on titania with the appearance of nonmetallic properties," *Science*, vol. 281, no. 5383, pp. 1647–1650, 1998.

[31] G. A. Ozin, J. G. McCaffrey, D. F. McIntosh et al., "Activation of dihydrogen and methane by photoexcited manganese and iron atoms in low temperature matrices," *Pure and Applied Chemistry*, vol. 56, no. 1, pp. 111–128, 1984.

[32] J. M. Parnis, S. A. Mitchell, J. García-Prieto, and G. A. Ozin, "Activation of methane by photoexcited copper atoms and the photochemistry of methylcopper hydride in solid methane matrices," *Journal of the American Chemical Society*, vol. 107, no. 26, pp. 8169–8178, 1985.

[33] G. A. Ozin, J. G. McCaffrey, and J. M. Parnis, "Photochemistry of transition-metal atoms: reactions with molecular hydrogen and methane in low-temperature matrices," *Angewandte Chemie*, vol. 25, no. 12, pp. 1072–1085, 1986.

[34] J. M. Parnis and G. A. Ozin, "Photochemical reactions of matrix-isolated aluminum atoms with methane and molecular hydrogen. 1. Methane," *Journal of Physical Chemistry*, vol. 93, no. 4, pp. 1204–1215, 1989.

[35] J. M. Parnis and G. A. Ozin, "Photochemical reactions of matrix-isolated aluminum atoms with methane and molecular hydrogen. 2. Molecular hydrogen," *Journal of Physical Chemistry*, vol. 93, no. 4, pp. 1215–1220, 1989.

[36] J. M. Parnis and G. A. Ozin, "Photochemical reactions of matrix-isolated aluminum atoms with methane and molecular hydrogen. 3. Structure, bonding, and reactivity," *Journal of Physical Chemistry*, vol. 93, no. 4, pp. 1220–1225, 1989.

[37] J. M. Parnis and G. A. Ozin, "Photochemistry of methylcopper hydride, CH3CuH: wavelength dependence of the product distribution," *Journal of Physical Chemistry*, vol. 93, no. 10, pp. 4023–4029, 1989.

[38] S. A. Mitchell, P. A. Hackett, D. M. Rayner, and M. Flood, "Branching ratios for chemical reaction in collisional quenching of excited $5s^{12}$ $S_{1/2}$ gallium atoms," *The Journal of Chemical Physics*, vol. 86, no. 12, pp. 6852–6861, 1987.

[39] D. A. Hensher and K. J. Button, *Handbook of Transport and the Environment*, Emerald Group Publishing, 2003.

[40] J. H. Pacheco-Sánchez, *Ab initio studies for C–H bond breaking of the methane molecule (CH4) and for Si–H bond breaking of the silane molecule (SiH4)*, Ph.D. thesis, Universidad Autónoma Metropolitana, (UAM-A), 2004.

[41] M. Yasuda, Y. Onishi, M. Ueba, T. Miyai, and A. Baba, "Direct reduction of alcohols: highly chemoselective reducing system for secondary or tertiary alcohols using chlorodiphenylsilane with a catalytic amount of indium trichloride," *Journal of Organic Chemistry*, vol. 66, no. 23, pp. 7741–7744, 2001.

[42] S. Das, D. Addis, S. Zhou, K. Junge, and M. Beller, "Zinc-catalyzed reduction of amides: unprecedented selectivity and functional group tolerance," *Journal of the American Chemical Society*, vol. 132, no. 6, pp. 1770–1771, 2010.

[43] F. Lehmann and M. Scobie, "Rapid and convenient microwave-assisted synthesis of primary amines via reductive N-alkylation of methyl carbamate with aldehydes," *Synthesis*, no. 11, pp. 1679–1681, 2008.

[44] Y. Kanazawa and H. Nishiyama, "Conjugate reduction of α, β-unsaturated aldehydes with rhodium(bis-oxazolinylphenyl) catalysts," *Synlett*, no. 19, pp. 3343–3345, 2006.

[45] Y. Sumida, H. Yorimitsu, and K. Oshima, "Palladium-catalyzed preparation of silyl enolates from α, β- unsaturated ketones or cyclopropyl ketones with hydrosilanes," *Journal of Organic Chemistry*, vol. 74, no. 20, pp. 7986–7989, 2009.

[46] H. A. Malik, G. J. Sormunen, and J. Montgomery, "A general strategy for regiocontrol in nickel-catalyzed reductive couplings of aldehydes and alkynes," *Journal of the American Chemical Society*, vol. 132, no. 18, pp. 6304–6305, 2010.

[47] K. Sa-Ei and J. Montgomery, "Highly diastereoselective preparation of anti-1,2-diols by catalytic addition of alkynylsilanes to α-silyloxyaldehydes," *Organic Letters*, vol. 8, no. 20, pp. 4441–4443, 2006.

[48] G. S. Girolami, T. B. Rauchfuss, and R. J. Angelici, *Synthesis and Technique in Inorganic Chemistry*, University Science Books, Mill Valley, Calif, USA, 1999.

[49] R. Venkatasubramanian, R. T. Pickett, and M. L. Timmons, "Epitaxy of germanium using germane in the presence of tetramethylgermanium," *Journal of Applied Physics*, vol. 66, no. 11, pp. 5662–5664, 1989.

[50] E. Woelk, D. V. Shenai-Khatkhate, R. L. DiCarlo Jr. et al., "Designing novel organogermanium OMVPE precursors for high-purity germanium films," *Journal of Crystal Growth*, vol. 287, no. 2, pp. 684–687, 2006.

[51] A. H. Mahan, L. M. Gedvilas, and J. D. Webb, "Si-H bonding in low hydrogen content amorphous silicon films as probed by infrared spectroscopy and x-ray diffraction," *Journal of Applied Physics*, vol. 87, no. 4, pp. 1650–1658, 2000.

[52] F. C. Marques, P. Wickboldt, D. Pang, J. H. Chen, and W. Paul, "Stress and thermomechanical properties of amorphous hydrogenated germanium thin films deposited by glow discharge," *Journal of Applied Physics*, vol. 84, no. 6, pp. 3118–3124, 1998.

[53] W. A. Turner, S. J. Jones, D. Pang et al., "Structural, optical, and electrical characterization of improved amorphous hydrogenated germanium," *Journal of Applied Physics*, vol. 67, no. 12, pp. 7430–7438, 1990.

[54] R. A. Street, *Hydrogenated Amorphous Silicon*, Cambridge University Press, New York, NY, USA, 1991.

[55] J. Robertson, "Deposition mechanism of hydrogenated amorphous silicon," *Journal of Applied Physics*, vol. 87, no. 5, pp. 2608–2617, 2000.

[56] A. R. Badzian, P. K. Bachmann, T. Hartnett, T. Badzian, and R. Messier, "Amorphous hydrogenated carbon films," in *Proceedings of the E-MRS Meeting*, P. Koidl and P. Oelhafen, Eds., vol. 17, p. 63, Stasbourg, France, June 1987.

[57] F. Demichelis, M. Fanciulli, G. Kaniadakis et al., "Amorphous hydrogenated carbon films," in *Proceedings of the E-MRS*

Meeting, P. Koidl and P. Oelhafen, Eds., vol. 17, p. 213, Stasbourg, France, June 1987.

[58] J. Reyes-Mena, J. González-Hernandez, R. Asomoza et al., "Amorphous hydrogenated carbon films," in *Proceedings of the E-MRS Meeting*, P. Koidl and P. Oelhafen, Eds., vol. 17, p. 229, Stasbourg, France, June 1987.

[59] J. C. Angus, "Amorphous hydrogenated carbon films," in *Proceedings of the E-MRS Meeting*, P. Koidl and P. Oelhafen, Eds., vol. 17, p. 179, Stasbourg, France, June 1987.

[60] S. Castillo, E. Poulain, and O. Novaro, "A theoretical study of the photochemistry of methylcopper hydride: II. Formation and stability of the $HCuCH_3$ intermediate complex," *International Journal of Quantum Chemistry*, vol. 40, pp. 577–585, 1991.

[61] J. H. Wang, H. Umemoto, A. W. K. Leung, and W. H. Breckenridge, "Reactions of $Zn(4s4p\ ^3P_1)$ and $Cd(5s5p\ ^3P_1)$ with SiH_4," *Journal of Chemical Physics*, vol. 104, no. 23, pp. 9401–9407, 1996.

[62] J. Perrin, M. Shiratani, P. Kae-Nune, H. Videlot, J. Jolly, and J. Guillon, "Surface reaction probabilities and kinetics of H, SiH_3, Si_2H_5, CH_3, and C_2H_5 during deposition of a-Si:H and a-C:H from H_2, SiH_4, and CH_4 discharges," *Journal of Vacuum Science and Technology A*, vol. 16, no. 1, pp. 278–289, 1998.

[63] A. G. Ramirez and R. Sinclair, "Wear effects on microstructural features of amorphous-carbon thin films," *Surface and Coatings Technology*, vol. 94-95, pp. 549–554, 1997.

[64] C. Velasco-Santos, A. L. Martínez-Hernández, A. Consultchi, R. Rodríguez, and V. M. Castaño, "Naturally produced carbon nanotubes," *Chemical Physics Letters*, vol. 373, no. 3-4, pp. 272–276, 2003.

[65] T. Taguchi, M. Morikawa, Y. Hiratsuka, and K. Toyoda, "Amorphous hydrogenated carbon films," in *Proceedings of the E-MRS Meeting*, P. Koidl and P. Oelhafen, Eds., vol. 17, p. 123, Stasbourg, France, June 1987.

[66] W. M. M. Kessels, A. H. M. Smets, D. C. Marra, E. S. Aydil, D. C. Schram, and M. C. M. van de Sanden, "On the growth mechanism of a-Si:H," *Thin Solid Films*, vol. 383, no. 1-2, pp. 154–160, 2001.

[67] W. M. M. Kessels, R. J. Severens, A. H. M. Smets et al., "Hydrogenated amorphous silicon deposited at very high growth rates by an expanding $Ar\text{-}H_2\text{-}SiH_4$ plasma," *Journal of Applied Physics*, vol. 89, no. 4, pp. 2404–2413, 2001.

[68] K. Winer, "Chemical-equilibrium model of optimal a-Si:H growth from SiH_4," *Physical Review B*, vol. 41, no. 11, pp. 7952–7954, 1990.

[69] W. H. Breckenridge, "Activation of H-H, Si-H, and C-H bonds by nsnp excited states of metal atoms," *Journal of Physical Chemistry*, vol. 100, no. 36, pp. 14840–14855, 1996.

[70] B. L. Kickel and P. B. Armentrout, "Reactions of Fe+, Co+, and Ni+ with silane. Electronic state effects, comparison to reactions with methane, and M+-SiHx (x = 0-3) bond energies," *Journal of the American Chemical Society*, vol. 117, no. 2, pp. 764–773, 1995.

[71] B. L. Kickel and P. B. Armentrout, "Guided ion beam studies of the reactions of group 3 metal ions (Sc+, Y+, La+, and Lu+) with silane. Electronic state effects, comparison to reactions with methane, and M+-SiHx (x = 0-3) Bond Energies," *Journal of the American Chemical Society*, vol. 117, no. 14, pp. 4057–4070, 1995.

[72] A. Ferhati, T. B. McMahon, and G. Ohanessian, "Activation of silane by W+ in the gas phase: fourier-transform Ion cyclotron resonance and ab initio theoretical studies," *Journal of the American Chemical Society*, vol. 118, no. 25, pp. 5997–6009, 1996.

[73] P. E. M. Siegbahn, M. Svensson, and R. H. Crabtree, "A theoretical study of mercury photosensitized reactions," *Journal of the American Chemical Society*, vol. 117, no. 25, pp. 6758–6765, 1995.

[74] J. F. Harrod, T. Ziegler, and V. Tschinke, "Theoretical study of Cp2Ti(H)(SiH3) and Cp2TiSiH2 and their possible role in the polymerization of primary organosilanes," *Organometallics*, vol. 9, no. 4, pp. 897–902, 1990.

[75] T. D. Tilley and H. G. Woo, "Dehydrogenative polymerization of silanes to polysilanes by zirconocene and hafnocene catalysts. A new polymerization mechanism," *Journal of the American Chemical Society*, vol. 111, no. 20, pp. 8043–8044, 1989.

[76] G. W. Parshall, *Homogeneous Catalysis: the Application and Chemistry of Catalysis by Soluble Transition Metal Complexes*, John Wiley & Sons, New York, NY, USA, 1992.

[77] P. Braunstein and M. J. Knorr, "Reactivity of the metal-silicon bond in organometallic chemistry," *Journal of Organometallic Chemistry*, vol. 500, no. 1-2, pp. 21–38, 1995.

[78] E. C. Zybill and C.Y. Liu, "Metal silicon multiple bonds: new building blocks for organic synthesis," *Synlett*, vol. 7, pp. 687–699, 1995.

[79] F. C. Marques, P. Wickboldt, D. Pang, J. H. Chen, and W. Paul, "Stress and thermomechanical properties of amorphous hydrogenated germanium thin films deposited by glow discharge," *Journal of Applied Physics*, vol. 84, no. 6, pp. 3118–3124, 1998.

[80] S. Castillo, *Theoretical study of the methane activation by excited atoms of copper (^2S, ^2D, and ^{2}) and Zinc (^1S, ^1P, and ^3P)*, Ph.D. thesis, Universidad Nacional Autonoma de Mexico (UNAM), 1992.

[81] H. M. Luna-García, *Molecular studies about the reaction mechanism for the formation of metal-silicon and metal germanium materials*, Ph.D. thesis, Universidad Autonoma Matropolitana Unidad Azcapotzalco (UAM-A), 2003.

[82] J. H. Pacheco-Sánchez and O. Novaro, "Transition probabilities found for M + CH_4 reactions (M = zinc, copper)," *International Journal of Quantum Chemistry*, vol. 108, no. 10, pp. 1645–1652, 2008.

[83] J. H. Pacheco-Sánchez, S. Castillo, H. Luna-García, and O. Novaro, "Transition probabilities on Ga (^{2}, ^{2}S, and ^{2}) +CH_4 reactions," *Journal of Chemical Physics*, vol. 126, no. 10, Article ID 106103, 2007.

[84] O. Novaro, M. A. Pacheco-Blas, and J. H. Pacheco-Sánchez, "Avoided crossings in metal (M)—gas (X) reactions (M = Hg, and X = SiH4, GeH4) ," *Theoretical Chemistry Accounts*, vol. 126, no. 3, pp. 109–116, 2010.

[85] J. H. Pacheco-Sánchez, S. Castillo, H. Luna-García, and O. Novaro, "Landau-zener theory for avoided crossings applied to the gallium-silane reactions," *International Journal of Quantum Chemistry*, vol. 107, no. 15, pp. 3053–3060, 2007.

[86] A. Ramírez-Solís and S. Castillo, "C_{3v} versus C_{2v} Cd(^{1}S,^{3}P, ^{1}P)-CH_4 van der Waals complexes: a variational and perturbational multireference configuration interaction study," *The Journal of Chemical Physics*, vol. 98, no. 10, pp. 8065–8069, 1993.

[87] J. H. Pacheco-Sánchez, H. M. Luna-García, L. M. García-Cruz, and O. Novaro, "Transition probabilities for the Au (^{2}S, ^{2}D, and ^{2}P) with SiH_4 reaction," *Journal of Chemical Physics*, vol. 132, no. 4, Article ID 044301, 2010.

[88] M. A. Pacheco-Blas, O. A. Novaro, and J. H. Pacheco-Sánchez, "A theoretical approach to the photochemical activation of matrix isolated aluminum atoms and their reaction with methane," *Journal of Chemical Physics*, vol. 133, no. 17, Article ID 174307, 2010.

[89] H. Eyring, *Quantum Chemistry*, John Wiley & Sons, New York, NY, USA, 1944.

[90] L. Rosenkewitsch, "Zur theorie des Durchschlags von dielektriken," *Journal of Physics-USSR*, vol. 1, p. 426, 1932.

[91] F. Colmenares, J. G. McCaffrey, and O. Novaro, "Quenching of excited 1P1 state atomic zinc by molecular nitrogen: a matrix-isolation spectroscopy/quantum chemical calculation study," *Journal of Chemical Physics*, vol. 114, no. 22, pp. 9911–9918, 2001.

[92] J. H. Pacheco, A. Bravo, and O. Novaro, "An ab initio study of platinum hydrogen interaction," *Revista Mexicana de Fisica*, vol. 52, no. 5, pp. 394–397, 2006.

[93] C. E. Moore, *Atomic Energy Levels*, U.S. National Bureau of Standards, Washington, DC, USA, 1971.

[94] K. P. Huber and G. Herzberg, *Molecular Spectra and Molecular Structure IV. Spectra of Diatomic Molecules*, Van Nostran, Princeton, NJ, USA, 1979.

[95] S. Castillo, A. Ramírez-solís, and E. Poulain, "Theoretical study of the reaction of Cd(^{1}S, ^{3}P, ^{1}P) with the methane molecule," *International Journal of Quantum Chemistry*, vol. 48, no. 27, pp. 587–598, 1993.

[96] K. Lee, H. S. Son, S. C. Bae, and J. K. Ku, "Collisional quenching of Ga(5p) atoms by H_2, D_2 and CH_4," *Chemical Physics Letters*, vol. 288, no. 2–4, pp. 531–537, 1998.

[97] M. Kronekvist, A. Langerquist, and H. Neuhaus, "The $A^1\Pi - {}^1\Sigma^+$ transition in the spectra of GaH and GaD," *Journal of Molecular Spectroscopy*, vol. 39, no. 3, pp. 516–518, 1971.

[98] H. J. Himmel, A. J. Downs, and T. Greene, "Reactions of ground state and electronically excited atoms of main group elements: a matrix perspective," *Chemical Reviews*, vol. 102, no. 11, pp. 4191–4241, 2002.

[99] P. R. Kemper, J. Bushenell, M. T. Bowers, and G. I. Gellene, "Binding between ground-state aluminum ions and small molecules: $A1^+ \cdot (H_2/CH_4/C_2H_2/C_2H_4/C_2H_6)_n$. Can Al^+ insert into H_2?" *Journal of Physical Chemistry A*, vol. 102, no. 44, pp. 8590–8597, 1998.

[100] M. A. Lefcourt and G. A. Ozin, "Aluminum(2P)-silane complex and photoreversible oxidative addition/reductive elimination reaction Al(2P){SiH4} .tautm. SiH3AlH. 1. Al(2P){SiH4} complex," *Journal of Physical Chemistry*, vol. 95, no. 7, pp. 2616–2623, 1991.

[101] G. A. Ozin, D. F. McIntosh, S. A. Mitchell, and J. García-Prieto, "Methane activation. Photochemical reaction of copper atoms in solid methane," *Journal of the American Chemical Society*, vol. 103, no. 6, pp. 1574–1575, 1981.

[102] J. M. Parnis and G. A. Ozin, "Photochemistry of methylcopper hydride, CH3CuH: wavelength dependence of the product distribution," *Journal of Physical Chemistry*, vol. 93, no. 10, pp. 4023–4029, 1989.

[103] R. A. Poirier, G. A. Ozin, D. F. McIntosh, I. G. Csizmadia, and R. Daudel, "Structure and bonding of H3CCuH," *Chemical Physics Letters*, vol. 101, no. 3, pp. 221–228, 1983.

[104] G. A. Ozin and J. G. McCaffrey, "Photoinduced reductive elimination of iron atoms and methane from CH3FeH," *Journal of the American Chemical Society*, vol. 104, no. 25, pp. 7351–7352, 1982.